Applied Physics Letters ARTICLE scitation.org/journal/apl

Prediction of the effects of rf irradiation on the I–V curves of a CDW compound

Cite as: Appl. Phys. Lett. **118**, 213106 (2021); doi: 10.1063/5.0051314
Submitted: 24 March 2021 · Accepted: 26 April 2021 ·
Published Online: 26 May 2021

S. A. Nikonov, S. G. Zybtsev, A. A. Maizlakh, and V. Ya. Pokrovskii[a)]

AFFILIATIONS

Kotelnikov Institute of Radioengineering and Electronics of RAS, 125009 Moscow, Russia

Note: This paper is part of the APL Special Collection on Charge-Density-Wave Quantum Materials and Devices.
[a)]**Author to whom correspondence should be addressed:** vadim.pokrovskiy@mail.ru

ABSTRACT

The Shapiro steps (ShSs) developing in sliding charge-density wave (CDW) under rf irradiation are considered in terms of the CDW travel in the periodic (washboard) potential. We demonstrate that treating the CDW as an inertialess object whose velocity is defined by the instantaneous voltage one can predict the positions of the ShSs in dc voltages for the given amplitude of rf voltage. Moreover, the approximation allows indicating the rf voltages at which the ShSs' magnitudes show maxima and minima. The only information necessary in advance is the I–V characteristic without rf irradiation and the cross-sectional area of the sample. Thus, one can recover the course of an I–V curve in average and the positions of ShSs on it, though not their forms.

The well-known feature of quasi one-dimensional conductors is the charge-density wave (CDW) forming below the temperature T_P of the so-called Peierls transition.[1,2] Under dc electric voltage, V_{dc}, exceeding the threshold, V_t, the CDWs can slide providing collective electronic dc current I_{CDW} with an ac component on top reflecting a periodic modulation of the CDW velocity. Both the threshold and the velocity modulation reveal the periodic pinning potential, known also as the washboard potential (WP). The period of WP usually coincides with λ, the CDW wavelength. If the sliding velocity is v, the frequency of the ac component equals v/λ, known as the fundamental, or washboard, frequency of CDW sliding, f_f.

An external rf voltage at frequency f can induce synchronization of the CDW sliding: in some range of V_{dc} values, at which f_f is close to f or one of its harmonics or subharmonics, the rf voltage dictates the velocity of CDW sliding: $f_f = if$, where i is the number of the harmonic.[3] In the synchronized modes, the CDW advances by $i\lambda$ within each period of rf voltage, $1/f$. The ranges of $I_{CDW} = \text{const}$ on the I–V curves known as Shapiro steps (ShSs) can be seen as pronounced dips of differential conductivity, $\sigma_d \equiv dI/dV_{dc}$, on the $\sigma_d(V_{dc})$ curves.

The wide spectrum of non-linear phenomena intrinsic to sliding CDWs is drawing interest to the quasi one-dimensional conductors from the applied point of view. The crystals with CDWs can work as mixing elements, switchers, memory elements,[4] and MOSFET-like structures.[5] Their electromechanical features,[6] namely, enormous drop of elastic moduli[7] and deformations under electric field,[8] open new space for applied challenges.

Typically, CDW conductors grow as whiskers and are natural nanoscale objects. Thicker crystals are easily cleaved down to nanometer-scale transverse dimensions. However, their shape is inconvenient for industrial manipulations. Fabrication of films[9–11] including oriented ones[12,13] can make a technological breakthrough, as well as involving intrinsically 2D sliding CDWs.[14,15]

In the context of the present Letter relevant are the applications of conductors with sliding CDWs as nanosized sources and receivers of rf irradiation with spectral resolution.[3] As a model material, we are taking the monoclinic phase of NbS_3 with CDW formed at $T_{P1} = 360$ K. The specifics of this compound are the unique combination of extreme coherence of CDW sliding and room-temperature operation.[1,16,17] The potential possibility of CDW synchronization at frequencies up to 200 GHz was claimed in Ref. 18. In Ref. 19, detection of rf voltage at T up to 360 K was demonstrated, temperature-independent current–frequency calibration was suggested. Involving another CDW existing in NbS_3, one can expand the working range up to 465 K.[20]

The rf receivers with spectral resolution are supposed to be based on the frequency dependence of the ShSs positions in I_{CDW} and the amplitude dependence of their magnitudes. We must note here that the magnitudes of ShSs are non-linear in V_{rf}, the rms value of the rf voltage. Moreover, their widths and amplitudes show aperiodic

oscillations in V_{rf}[22,23] and are usually approximated with the Bessel function, by analogy with similar oscillations in Josephson junctions (JJs).[24] These oscillations are in the focus of the present Letter. For definiteness, we will treat the ShSs magnitudes in terms of their widths, δV^*_i, where i is the No of the ShS. We determine δV^*_i as the width of a rectangle with upper side at σ equal to σ_d beyond the dip in $\sigma_d(V)$, the lower side at $\sigma = \sigma_d(0)$, and having the same area as the original dip.[25]

A special case is the segment of an I–V curve in the range of $|V| < V_t$, where $I_{CDW} = 0$. Below, for generality of consideration, we refer to this segment as the 0th ShS.[25] Then, the width of this ShS, δV^*_0, is approximately $2V_t$.

A somewhat overlooked fact is that, as a rule, the rf frequencies across the sample are low in comparison with inverse relaxation times of the CDW sliding: the "pinning frequencies" of the CDWs lie in the GHz range (Refs. 1, 2, 21 and references therein). Consequently, the instantaneous velocity of the CDW under mixed dc+rf voltage, $v(t)$, at any point of time is approximately defined by the instantaneous value of voltage, $V(t)$, and, thus, can be found based on the I–V curve measured under purely dc voltage.

Further, knowing $v(t)$ one can find the CDW displacement on the microscopic time scales, comparable with $1/f_f$. Recently, this approach allowed description of oscillations of δV^*_i as a function of CDW travel in either of the half-periods of the rf voltage, $1/(2f)$. The oscillations appear periodic, the period being equal to λ.[25] It is important that the origin of the WP, that is, the mechanism of CDW pinning and sliding, is inessential for this conclusion.

The instantaneous-velocity model considering v as a function solely of V does not take into account the variations of the CDW velocity in the WP. These variations impose a certain limitation on the area and accuracy of model implementation. Luckily, in Ref. 25 the calculations were focused on the minima of the ShSs magnitudes, and in these modes, the CDW travels by integer number of λ in either half-period of the rf voltage. In this case, the velocity variations are averaged out.

In this Letter, we probe the capabilities of the "instantaneous-velocity" approach in description of the features of the I–V curves of CDW conductors subjected to rf voltage. All the measurements are performed on the monoclinic NbS_3 at room temperature. We demonstrate that the approach provides the basic features of the I–V curves under rf irradiation. In particular, given an I–V curve without irradiation one can predict the dc voltages of the ShSs for any V_{rf} value. One can also indicate the rf voltages at which the ShSs show minima or maxima. Also, the approach gives the form of the I–V curves in average; however, it cannot reconstruct the ShSs, because their origin roots in the non-uniformity of the CDW sliding in the WP.

The details of the experiment can be found in Ref. 25. In the present studies, we are considering the NbS_3 sample with dimensions $20\,\mu m \times 1.4 \times 10^{-2}\,\mu m^2$. In Ref. 25, for simplicity, we reduced the effect of the sine-wave voltage to the effect of square-wave signal with the same rms magnitude, V_{rf}. Here, we escape this simplification: the CDW travel is calculated as an integral of $v(t)$ with respect to t.

Figure 1 shows a set of "differential" I–V curves, σ_d vs V_{dc}, under 75 MHz irradiation with V_{rf} increasing from 0 (the bottom curve) to 0.9 V (the upper curve) (see Fig. 2 from Refs. 25).[26] One can see the oscillations of the widths of ShSs No 0–3.

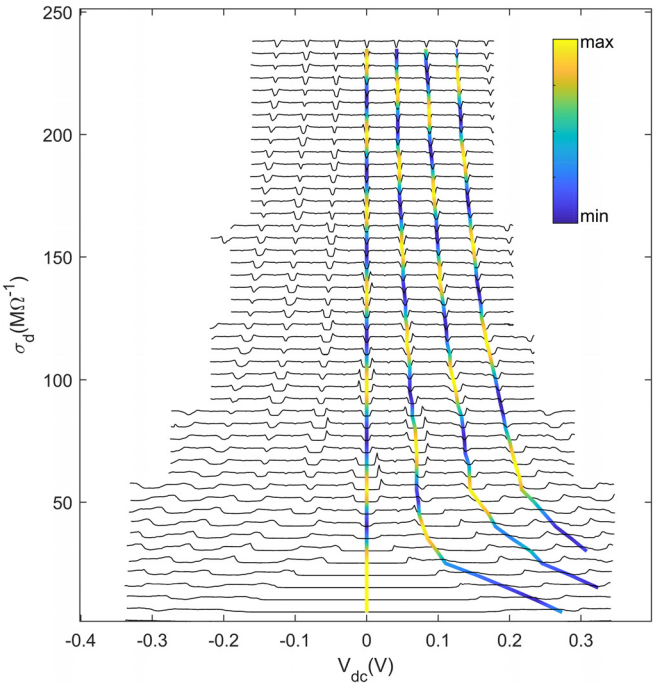

FIG. 1. A set of σ_d vs V_{dc} curves under sine-wave rf irradiation with V_{rf} increasing from 0 to the maximum value (the upper curve). The V_{rf} values across the sample are 0, 74, 148, 197, 246, 296, 320, 345, 369, 394, 419, 443, 456, 468, 480, 493, 505, 517, 530, 542, 554, 567, 579, 591, 603, 616, 628, 640, 653, 665, 677, 690, 702, 714, 727, 739, 751, 764, 776, 788, 800, 813, 825, 837, 850, 862, 874, and 887 mV. All the curves, except for the lower one, are shifted upward in increments of 6.8 $M\Omega^{-1}$. $f = 75$ MHz. The calculated V_{dc} values for $i = 0$, 1, 2, and 3 are shown on top and are connected with solid straight lines. The colors of the lines scale the variation of the ShSs magnitudes between minima and maxima (see the color map).

Figures 2(a) and 2(b) repeat Figs. 4(b) and 9 from,[25] respectively, with the CDW travel calculated using numerical integration of $v(t)$. The oscillations of the ShSs magnitudes, δV^*_i,[25] appear periodic with better accuracy than in Ref. 25, which is most visible for the high numbers of oscillations, that is, higher V_{dc} [Fig. 2(a)]. The "control sums" of the ShSs, that is, the calculated total travels of the CDW in both half-periods of the rf voltage, appear closer to the expected values: λ for the first ShS, 2λ—for the second one, and 3λ—for the third one [Fig. 2(b)]. Better accuracy is achieved at higher V_{rf}.

Now we are turning to the inverse problem: the determination of the dc voltages of the ShSs and of their magnitudes for given V_{rf}. We are basing only on the I–V curve of the non-irradiated sample together with its I_{CDW}/f_f ratio. This ratio is defined by the number of CDW-carrying chains in the sample, that is, by the cross-sectional area of the sample.[16,17] In practice, we determined I_{CDW}/f_f, as well as the cross-sectional area, from the non-linear current at the first ShS.

Figure 3 shows the $I(V)$ characteristic of the same sample without irradiation (see the bottom curve in Fig. 1), the basic one for further processing. It is important that it is measured in a wider voltage range (not completely shown in Fig. 3).[27] From this curve for any given voltage, one can find I_{CDW} as the non-linear current. At given V_{dc} and V_{rf},

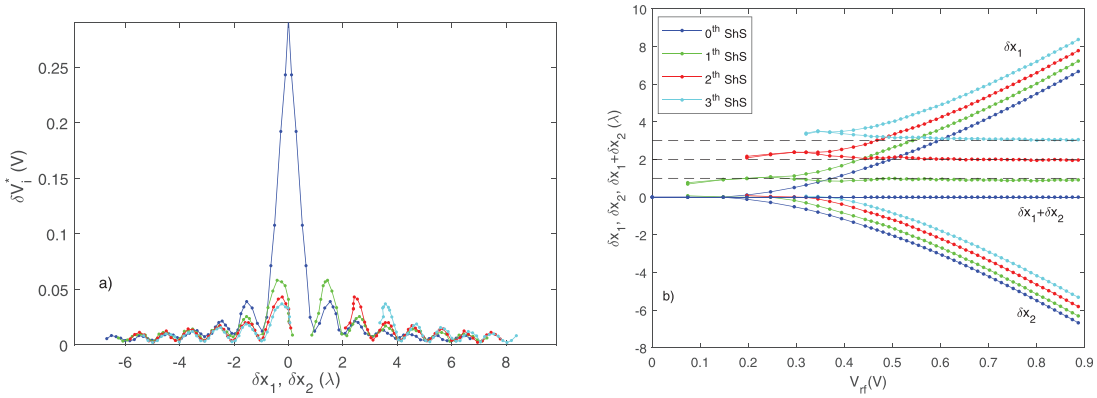

FIG. 2. (a) δV^*_i ($i = 0$–3) vs δx_1 (the positive values) and δx_2 (the negative or 0 values); b) δx_1, δx_2 and $\delta x_1+\delta x_2$ vs rf voltage. δx_1 and δx_2 are calculated for the $\sigma_d(V_{dc})$ curves in Fig. 1; the voltages in the centers of the ShSs are taken. The broken lines show the "control sums," that is, the values of $\delta x_1+\delta x_2$ known in advance. The values of δx_1 and δx_2 were calculated as integrals of $v(t)$ with respect to t.

we take the instantaneous voltage $V(t) = V_{dc}+\sqrt{2}V_{rf}\sin(2\pi ft)$. Then, the CDW advancement in time can be calculated as

$$\delta x = \lambda\int f_f(t)dt = 1\int\left[I_{CDW}(t)/(I_{CDW}/f_f)\right]dt$$
$$= \lambda\int\left[I_{CDW}(V_{dc}+\sqrt{2}V_{rf}\sin(2\pi ft)/(I_{CDW}/f_f)\right]dt.$$

For the present sample, $I_{CDW}/f_f = 2.54$ nA/MHz. To find the voltages of ShSs for given V_{rf}, we at first calculated the CDW advancement in the first and second half-periods of rf voltage, δx_1 and δx_2,[28] as a function of V_{dc}. δx_1, was found integrating over the time interval $0 < t < 1/(2f)$. Correspondingly, δx_2 was found integrating over the time interval $1/(2f) < t < 1/f$. Then, V_{dc} was fit to match the condition $\delta x_1+\delta x_2 = i\lambda$, where i is the ShS number.[29]

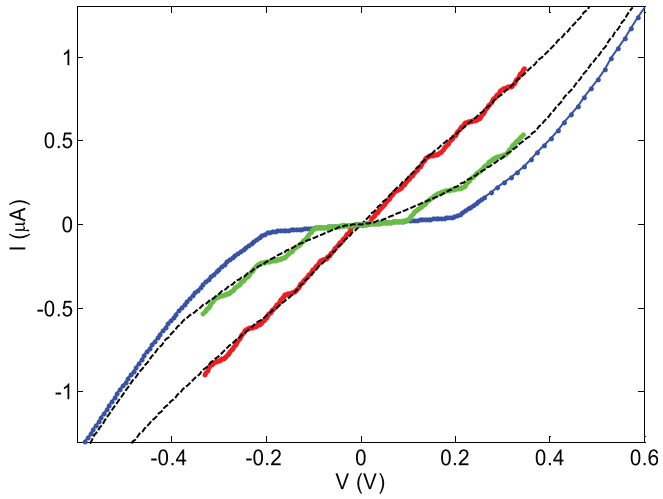

FIG. 3. The I–V curves of the representative sample at $V_{rf} = 0$, 246 mV, and 443 mV (see the curves No. 1, 5, and 12 from Fig. 1, counting from the bottom). The broken lines show the results of calculation based on the I–V curve at $V_{rf} = 0$.

The result of the calculation of V_{dc} of the ShSs for $i = 1$, 2, 3 is shown in Fig. 1 with points on top of the $\sigma_d(V)$ curves with $V_{rf} \neq 0$. To make the result more visual, we connected the points with solid straight lines crossing the curves. One can see that the resulting polyline[30] fairly shows the positions of the ShSs.

The next step is to indicate the minima of the ShSs amplitudes. The first minimum of the first ShS must meet the condition on the total CDW *travel*, δx_1-$\delta x_2 = 3\lambda$.[25,29] For the following minima, the conditions are as follows: δx_1-$\delta x_2 = 5\lambda$, 7λ, etc. These points are marked with dark blue in Fig. 1. As we noted above, in these cases δx_1 and δx_2 equal to integer numbers of λ; therefore, the conditions for the minima are more exact. For the maxima of the first ShS, we took the condition δx_1-$\delta x_2 = 2\lambda$, 4λ, etc. These points are marked with bright yellow. Finally, the change of ShSs' magnitudes between maxima and minima is illustrated by the gradual changes of color in between (see the color map). With this color scale, one can see that the model can predict the variation of the ShSs magnitudes vs rf voltage.

The minima for the second ShS were calculated from the conditions δx_1-$\delta x_2 = 4\lambda$, 6λ, etc., for the third ShS—from the conditions δx_1-$\delta x_2 = 5\lambda$, 7λ, etc.[25] The maxima were supposed to be halfway between the minima. The position of the 0th ShS is at $V = 0$ in any case ($\delta x_1+\delta x_2 = 0$), while its minima and maxima can be found from the conditions $\delta x_1 = 1$, 2, 3… and δx_1=1.5, 2.5, 3.5…, respectively. The resulting variation of V_t is shown with the color of the vertical line at $V = 0$.

To comprehend the scope of application of the "instantaneous-velocity" model, we tried to reconstruct the whole I–V curve under rf irradiation basing only on the I–V curve of the non-irradiated sample.

In Fig. 3, in addition to the "basic" $I(V)$ dependence, we plotted the I–V curves for two rf voltages: 246 mV and 443 mV (No 5 and 12 from Fig. 1). The broken lines on top of them show the results of reconstruction based on the $I(V)$ curve at $V_{rf} = 0$. To obtain a point, we took the time integral of $I[V_{dc}+\sqrt{2}V_{rf}\sin(2\pi ft)]$ from 0 to $1/f$ and divided the resulting charge by $1/f$. The only fitting parameter was V_{rf}, and it coincided with the experimental values of V_{rf} within 3%.

Of course, the model does not recover the ShSs *per se*. One gets monotonic growth of CDW current with V, while the ShSs, where $dI_{CDW}/dV = 0$, intrinsically originate from the non-uniform sliding of

the CDW in the WP. In all the cases, the fits cross the ShSs near their centers, regardless of whether the ShS width is close to its maximum or minimum. From this, as well as from Fig. 2(b), one can conclude that the condition of $\delta x_{1,2}/\lambda$ to be integer is not so crucial for the "instantaneous velocity" model.

Another notable discrepancy of the calculations with the experiment is seen at low V_{rf} values. In Fig. 1, the solid curves cross the left edges of the ShSs rather than their centers. Correspondingly, in Fig. 2(b) the "control sums" for the first ShS notably exceed λ, for the second exceed 2λ, and for the third exceed 3λ. This mismatching can be attributed to the inaccuracy of the model at low voltages. In particular, in the range of $|V(t)|<V_t$ the CDW is considered as resting, while actually it is moving within a WP valley. When $V<0$, the CDW is moving backward, and therefore, its total displacement can be overestimated [Fig 2(b)], and the experimental V_{dc} values of the ShSs centers appear somewhat higher than the calculated ones (Fig. 1).

In addition, we must note that the model can be applied to the oscillation of *subharmonic* ShSs and of the *satellites* of the ShSs appearing in the case of mixing two frequencies in a CDW system. The experiment on frequency mixing will be published in separate article.[31]

In summary, the "instantaneous-velocity" model, implying inertialess response of the CDW to the mixed dc+rf voltage and ignoring the velocity variation in the WP, appears successful in the treatment of the non-linear I–V curves of quasi one-dimensional conductors. Given the I–V curve of an unirradiated sample, the model predicts the shape of the I–V curve under rf irradiation with known V_{rf}. Though the model does not describe the form of the features at the ShSs, it allows indication of their positions in V_{dc}, as well as the values of V_{rf} at which the ShSs' magnitudes show maxima and minima.

The condition of minimum (maximum) is the CDW travel by integer (half-integer) number of wavelengths during either half-period of the rf voltage. These conditions make an immediate applied output. In Ref. 25, like in a number of other studies of CDWs under rf voltage, calibration of rf voltage across the samples required special efforts: typically, the samples are high-Ohmic and poorly match the rf source. Our result allows rf calibration based on the measurements of the I–V curves. For example, one can take the curve showing the first minimum of E_t. In this case, rf voltage induces the CDW oscillations around the potential minimum by $\pm\lambda/2$.[25] From this condition, one can calculate V_{rf} taking it as a fitting parameter. The ratio of the output rf voltage of the generator to the calculated V_{rf} will give the attenuation coefficient. In Ref. 31, this technique was successfully applied for the calibration of rf voltages at different frequencies.

The authors are grateful to S.V. Zaitsev-Zotov for the help in synthesis of high-quality crystals. The support of RFBR (Grant Nos. 20-02-00827 and 20-32-90231) is acknowledged.

DATA AVAILABILITY

The data that support the findings of this study are available from the corresponding author upon reasonable request.

REFERENCES

[1]P. Monceau, "Electronic crystals: An experimental overview," Adv. Phys. **61**, 325 (2012).
[2]G. Grüner, *Density Waves in Solids* (Addison-Wesley, Reading, MA, 1994).
[3]S. Brown and A. Zettl, in *Charge Density Wave Current Oscillations and Interference Effects, in Charge Density Waves in Solids*, edited by L. P. Gor'kov and G. Grüner (Elsevier, Amsterdam, North-Holland, 1989), Vol. 25, p. 223.
[4]R. E. Thorne, "Charge-density-wave conductors," Phys. Today **49**(5), 42 (1996).
[5]T. L. Adelman, S. Zaitsev-Zotov, and R. E. Thorne, "Field-effect modulation of charge-density-wave transport in $NbSe_3$ and TaS_3," Phys. Rev. Lett. **74**, 5264 (1995).
[6]V. Ya. Pokrovskii, S. G. Zybtsev, M. V. Nikitin, I. G. Gorlova, V. F. Nasretdinova, and S. V. Zaitsev-Zotov, "High-frequency, 'quantum' and electromechanical effects in quasi-one-dimensional charge density wave conductors," Phys.-Usp. **56**, 29–48 (2013).
[7]J. W. Brill, "Handbook of elastic properties of solids," in *Liquids and Gases*, edited by M. Levy (Academic Press, New York, 2001), Vol. 2, Chap. 10, p. 143.
[8]C. Day, "Whiskers of tantalum trisulfide twist in response to an electric field," Phys. Today **60**(7), 24 (2007).
[9]P. A. Poltarak, S. B. Artemkina, A. I. Bulavchenko, T. Y. Podlipskaya, and V. E. Fedorov, "Colloidal dispersions of tantalum trisulfide: Syntheses and characteristics," Russ. Chem. Bull. **64**, 1850 (2015).
[10]V. E. Fedorov, S. B. Artemkina *et al.*, "Colloidal solutions of niobium trisulfide and niobium triselenide," J. Mater. Chem. C **2**, 5479 (2014).
[11]J. O. Island *et al.*, "Electronics and optoelectronics of quasi-1D layered transition metal trichalcogenides," 2D Mater. **4**, 022003 (2017).
[12]H. S. J. van der Zant, O. C. Mantel, C. Dekker, J. E. Mooij, and C. Traeholt, "Thin film growth of the charge-density-wave oxide $Rb_{0.3}0MoO_3$," Appl. Phys. Lett. **68**, 3823 (1996).
[13]D. Dominko, D. Starešinić, K. Salamon, K. Biljaković, A. Tomeljak *et al.*, "Detection of charge density wave ground state in granular thin films of blue bronze $K_{0.3}MoO_3$ by femtosecond spectroscopy," J. Appl. Phys. **110**, 014907 (2011).
[14]G. Liu, S. Rumyantsev, M. A. Bloodgood, T. T. Salguero, and A. A. Balandin, "Low-frequency current fluctuations and sliding of the charge density waves in two-dimensional materials," Nano Lett. **18**, 3630 (2018).
[15]A. A. Sinchenko, P. Lejay, and P. Monceau, "Sliding charge-density wave in two-dimensional rare-earth tellurides," Phys. Rev. B **85**, 241104(R) (2012).
[16]S. G. Zybtsev, V. Y. Pokrovskii, V. F. Nasretdinova, and S. V. Zaitsev-Zotov, "Gigahertz-range synchronization at room temperature and other features of charge-density wave transport in the quasi-one-dimensional conductor NbS_3," Appl. Phys. Lett. **94**, 152112 (2009).
[17]S. G. Zybtsev, V. Y. Pokrovskii, V. F. Nasretdinova, S. V. Zaitsev-Zotov, V. V. Pavlovskiy, A. B. Odobesco, W. W. Pai, M.-W. Chu, Y. G. Lin, E. Zupanič, H. J. P. van Midden, S. Šturm, E. Tchernychova, A. Prodan, J. C. Bennett, I. R. Mukhamedshin, O. V. Chernysheva, A. P. Menushenkov, V. B. Loginov, B. A. Loginov, A. N. Titov, and M. Abdel-Hafiez, "NbS_3—A unique quasi one-dimensional conductor with three charge density wave transitions," Phys. Rev. B **95**, 035110 (2017).
[18]S. G. Zybtsev, V. Y. Pokrovskii, S. V. Zaitsev-Zotov, and V. F. Nasretdinova, "Growth, crystal structure and transport properties of one-dimensional conductors NbS_3," Physica B **407**, 1696–1699 (2012).
[19]S. G. Zybtsev, S. A. Nikonov, and V. Y. Pokrovskii, "Spontaneous phase slippage and CDW synchronization near the Peierls transition," Phys. Rev. B **102**, 235415 (2020).
[20]S. G. Zybtsev, V. Y. Pokrovskii, V. F. Nasretdinova, S. V. Zaitsev-Zotov, E. Zupanič, M. van Midden, and W. W. Pai, "The ultra-high-TP charge-density wave in the monoclinic phase of NbS_3," J. Alloys Compd. **854**, 157098 (2021).
[21]D. Reagor, S. Sridhar, M. Maki, and G. Grüner, "Inertial charge-density-wave dynamics in $(TaSe_4)_2I$," Phys. Rev B **32**, 8445 (1985).
[22]A. Zettl and G. Grüner, "Phase coherence in the current-carrying charge-density-wave state: Ac-dc coupling experiments in $NbSe_3$," Phys. Rev. B **29**, 755 (1984).
[23]R. E. Thorne, W. G. Lyons, J. W. Lyding, J. R. Tucker, and J. Bardeen, "Charge-density-wave transport in quasi-one-dimensional conductors. II. Ac-dc interference phenomena," Phys. Rev. B **35**, 6360 (1987).
[24]S. Shapiro, A. Janus, and S. Holly, "Effect of microwaves on Josephson currents in superconducting tunneling," Rev. Mod. Phys. **36**, 223 (1964).
[25]S. G. Zybtsev, S. A. Nikonov, V. Ya. Pokrovskii, V. V. Pavlovskiy, and D. Starešinić, "Step-by-step advancement of the charge-density wave in the rf-synchronized modes and oscillations of the width of Shapiro steps with respect to the rf power applied," Phys. Rev. B **101**, 115425 (2020).

[26]The step in V_{rf} is 12 mV for $V_{rf} > 420$ mV and larger for small V_{rf} values. The correct values of V_{rf} valid also for Fig. 2 from Ref. 25, are indicated in the caption to Fig. 1.

[27]Under rf irradiation the instantaneous voltage at each V value varies from $V+\sqrt{2}V_{rf}$ to $V-\sqrt{2}V_{rf}$. Therefore for consideration of the curves in Fig. 1 the range of V_{dc} is to be by $\sqrt{2}V_{rf}$ wider in both directions.

[28]We consider the half-period in which the signs of V_{dc} and rf voltage coincide as the first one. During the second half-period the signs are opposite.

[29]While δx_1 is positive, δx_2 is typically negative or zero.[25] Therefore, the total CDW displacement in $1/f$ time interval, $\delta x_1+\delta x_2$, equals $|\delta x_1|-|\delta x_2|$, while the total travel, $|\delta x_1|+|\delta x_2|$, equals $\delta x_1-\delta x_2$.

[30]In principle, V_{dc} can be calculated for an arbitrary V_{rf}, so that the polyline can be made smooth.

[31]S. A. Nikonov, S. G. Zybtsev, and V. Y. Pokrovskii, "RF Mixing with sliding charge-density waves," Appl. Phys. Lett. (to be published).